FMOS: the fiber multiple-object spectrograph VI: on board performances and results of the engineering observations

Fumihide Iwamuro[a], Toshinori Maihara[a], Masayuki Akiyama[b], Masahiko Kimura[c], Naoyuki Tamura[c], Naruhisa Takato[c], Kouji Ohta[a], Shigeru Eto[a], Yuuki Moritani[a], Gavin B. Dalton[d], Ian J. Lewis[d], Hanshin Lee[d], Ian A. J. Tosh[e], Tim R. Froud[e], Graham J. Murray[f], Colin Blackburn[f], David G. Bonfield[g], Peter R. Gillingham[h], Scott Smedley[h], Greg A. Smith[h], and Gabriella Frost[h]

[a]Department of Astronomy, Kyoto University, Kitashirakawa, Kyoto, Japan;
[b]Astronomical Institute, Tohoku University, Aramaki, Sendai, Japan;
[c]Subaru Telescope, National Astronomical Observatory of Japan, Hilo, HI, USA;
[d]Department of Physics, University of Oxford, Keble Road, Oxford, UK;
[e]STFC Rutherford Appleton Laboratory, Chilton, Didcot, Oxfordshire, UK;
[f]Department of Physics, University of Durham, South Road, Durham, UK;
[g]ORAU/Goddard Space Flight Center, Greenbelt, MD, USA;
[h]Anglo-Australian Observatory, P.O. Box 296, Epping, NSW, Australia

ABSTRACT

FMOS: the Fiber Multiple-Object Spectrograph is the next common-use instrument of the Subaru Telescope, having a capability of 400 targets multiplicity in the near-infrared 0.9−1.8μm wavelength range with a field coverage of 30′ diameter. FMOS consists of three units: 1) the prime focus unit including the corrector lenses, the Echidna fiber positioner, and the instrument-bay to adjust the instrument focus and shift the axis of the corrector lens system, 2) the fiber bundle unit equipping two fiber slits on one end and a fiber connector box with the back-illumination mechanism on the other end on the bundle, 3) the two infrared spectrographs (IRS1 and IRS2) to obtain 2×200 spectra simultaneously. After all the components were installed in the telescope at the end of 2007, the total performance was checked through various tests and engineering observations. We report the results of these tests and demonstrate the performance of FMOS.

Keywords: Infrared, Spectrograph, Fiber

1. INTRODUCTION

The next common-use instrument of the Subaru Telescope, the Fiber Multiple-Object Spectrograph (FMOS)[1–3] is almost completed after 8 years of development. All the mechanical components: the prime focus unit[4] (PFU: Fig. 1) including the Echidna fiber positioner[5–7] and the corrector lenses,[8] the fiber bundle unit,[9] and the two infrared spectrographs called IRS1[10] and IRS2[11–13] (Fig. 2 and Fig. 3), were assembled and mounted on the telescope at the end of 2007. Since then the engineering observations have been carried out for three times (December 2007, January and May 2008) to check the basic capability of the system with the full mechanical configuration. Although another engineering observation was scheduled in February, it was canceled owing to unexpected leakage of the coolant inside of the Echidna. Several other engineering observations are required before opening the system to common use from the later half of 2009. In this paper, after brief description of the required items during the engineering observations in section 2, the results are reported with typical images in section 3, and we discuss the expected performance as well as the current problem in section 4.

Further author information: (Send correspondence to F.I.)
F.I.: E-mail: iwamuro@kusastro.kyoto-u.ac.jp, Telephone: +81 75 753 3891

Ground-based and Airborne Instrumentation for Astronomy II, edited by Ian S. McLean, Mark M. Casali,
Proc. of SPIE Vol. 7014, 70140T, (2008) · 0277-786X/08/$18 · doi: 10.1117/12.787746

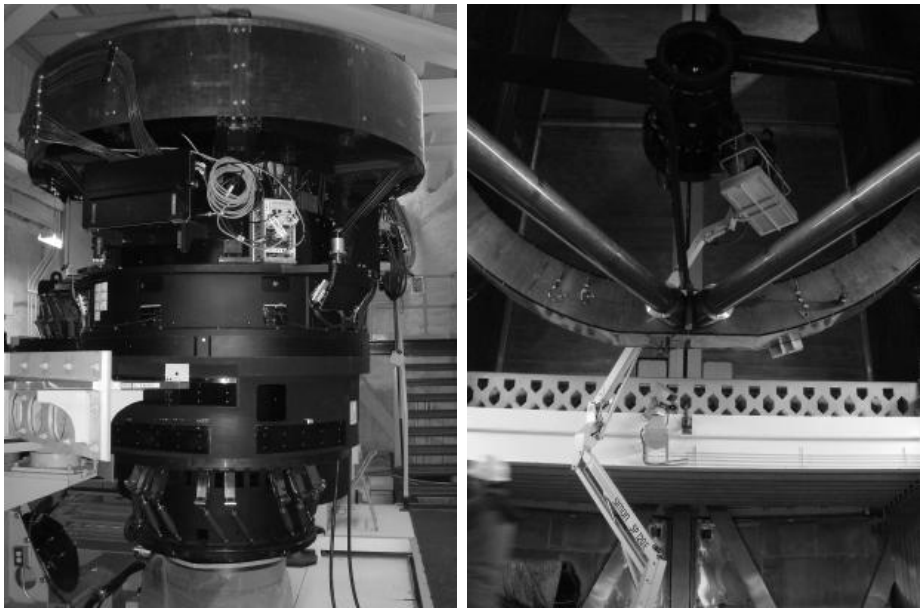

Figure 1. The prime focus unit (PFU) including the corrector lenses, the Echidna fiber positioner, and the instrument-bay to adjust the instrument focus and shift the axis of the corrector lens system (left). How to access the PFU while observations (right).

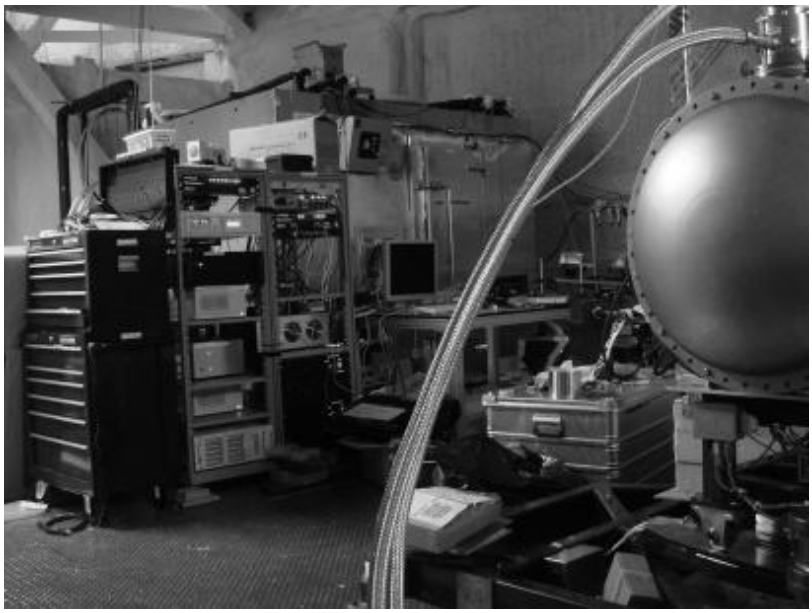

Figure 2. The infrared spectrograph IRS1 located parallel to IRS2 (near side).

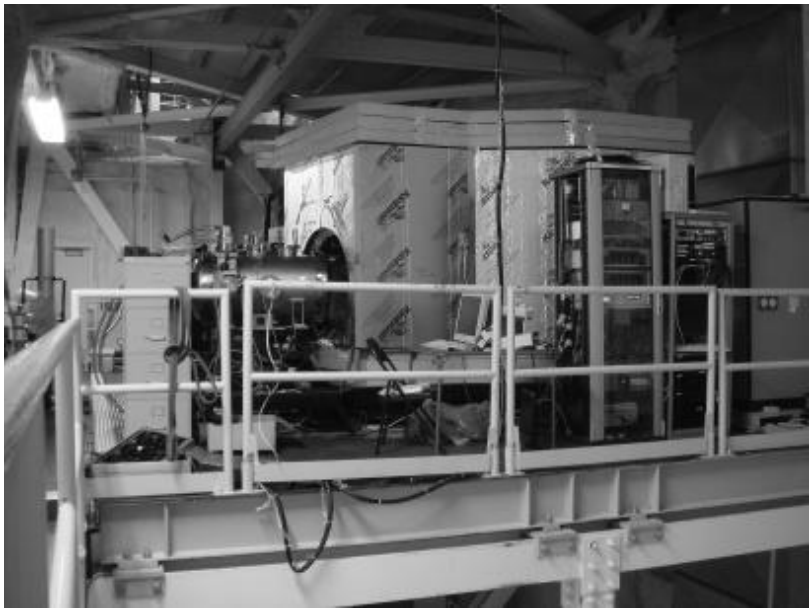

Figure 3. IRS2 installed in the 4th floor of the dome of the Subaru telescope.

2. ENGINEERING OBSERVATIONS

The primary purpose of the engineering observation is the verification of the basic performance of the instrument: 1) image quality of the prime focus through the corrector lenses, 2) pointing accuracy of the telescope with the FMOS PFU, 3) accuracy of the fiber configuration on the telescope and guiding stability using fiber bundles, and 4) total efficiency of the system compared with the expected value from the measurement of each component. The total system performance including the fiber configuration and the detector readout time is estimated from these results, which should be confirmed by the real observation of the faint objects at the end of the engineering observation.

Before verification of the image quality, we have to align the position of the corrector lenses with the axis of the primary mirror of the telescope minimizing the coma aberration of stellar images at several positions in the field taken by the sky camera installed in the Echidna unit. The aberration at the center of the field is also measured by the Shack-Hartmann camera in the PFU. After this adjustment, we measure the position of the instrument-rotator axis to determine the offset from the mechanical origin of the Echidna, and then the rough pointing analysis script of the telescope is executed. Next, we measure the image sizes and the positions of the bright stars in the field of $30'$ diameter again, to confirm the tilt and curvature of the focal plane in addition to mapping the distortion pattern of the field. Here, the prime focus is ready for the farther test of the Echidna by setting the focal plane parameters to the Echidna control software.

To check the accuracy of the fiber configuration, a part of the galactic plane (or an open cluster) is observed after the fiber configuration for the field. Focus position of the fibers can be confirmed using the images of the guide stars through guide fiber bundles. Since the focus position of the sky camera is not exactly the same as that of the Echidna fibers, we have to make a small offset to the focus position before exposures of the spectrographs. Next, we measure the count of each object taken by IRS1 and IRS2 with various small offsets of the field to make sure that all the fibers are configured at the best position. The exact focus position is also confirmed by checking the count of each spectra at various focus positions. In this observation, we can also determine the total efficiency of the system for point sources, which should be compared with that for uniform surface brightness using a blackbody source. At the best focus and field position, the guiding stability is tested for the assumed long exposure using the guide star images on the guide fiber bundles in addition to monitoring the count of each spectrum taken by the sequential short exposures of the spectrographs.

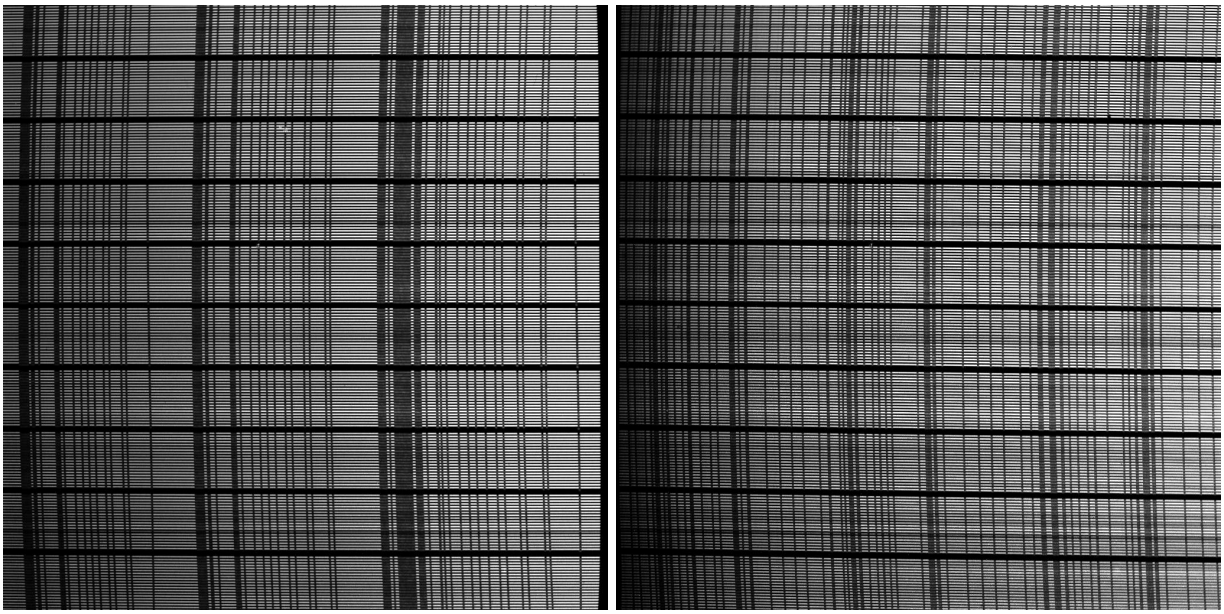

Figure 4. The blackbody spectra with a temperature of $1000^{\circ}C$ in the J-long (left), and H-short (right) wavelength range.

In the case of a scientific observation, beam switching is required for taking the sky spectra to subtract the background emission. Moreover, quick modification of the fiber configuration, "tweak", is also required among beam switching when appreciable differences between the fibers and the objects are expected. All these performance should be confirmed during the engineering observation. At the same time, the high level commands for the scheduled observation should be improved as well as the reduction software of the obtained spectra.

3. RESULTS

After the PFU is mounted on the telescope, all the cables and fibers are connected to boot up the system. We can check the total performance of the system only when the PFU is at the prime focus of the telescope, because we cannot connect fibers between the Echidna and the spectrographs when the Echidna at the rest position (at the top unit exchanger on the 4th floor of the dome). At first, a black body source with a temperature of $1000^{\circ}C$ was attached to the Cassegrain focus to measure the system efficiency. Fig. 4 is the black body spectra taken by IRS1 in the J-long ($1.13\sim1.35\mu$m) and H-short ($1.4\sim1.6\mu$m) wavelength range. The fiber slit consists of 10 subsets of 20 fibers separated with a small gap among them. Fig. 4 also shows the image of the airglow mask on the mask mirror reflecting a considerable flux because we have not blackened the mask yet. The typical FWHM of the vertical width of each spectrum is 5 pixels with a pitch of 10 pixels between the spectra. The direction of dispersion is slightly tilted in the H-short band caused by a small misalignment of the H-band mask mirror.

Fig. 5 shows the wavelength dependent efficiency for each spectrum except for the J-short ($0.91\sim1.13\mu$m) band, in which the optical configuration has not been fixed yet. The black body photons emitted from the Cassegrain focus go through the three primary corrector lenses, F/2 fibers in the Echidna unit, two relay lenses in the fiber connector box on the side panel of the PFU, F/5 fiber bundle with 60m long, and in the infrared spectrograph, seven reflective surfaces (including one grating) and eleven refractive optical elements (including one thermal cut filter) to the detector. Therefore the measured efficiency contains almost all the factor should be considered except for the reflectivity of the primary mirror, throughput of the sky, and the focal ratio dependency of the fiber input surfaces. The maximum throughput of 30% is almost consistent with the ideal value roughly estimated by the following calculation.

$$0.96^{(3+2+2+10)} \times 0.98^6 \times 0.90^3 = 0.32$$

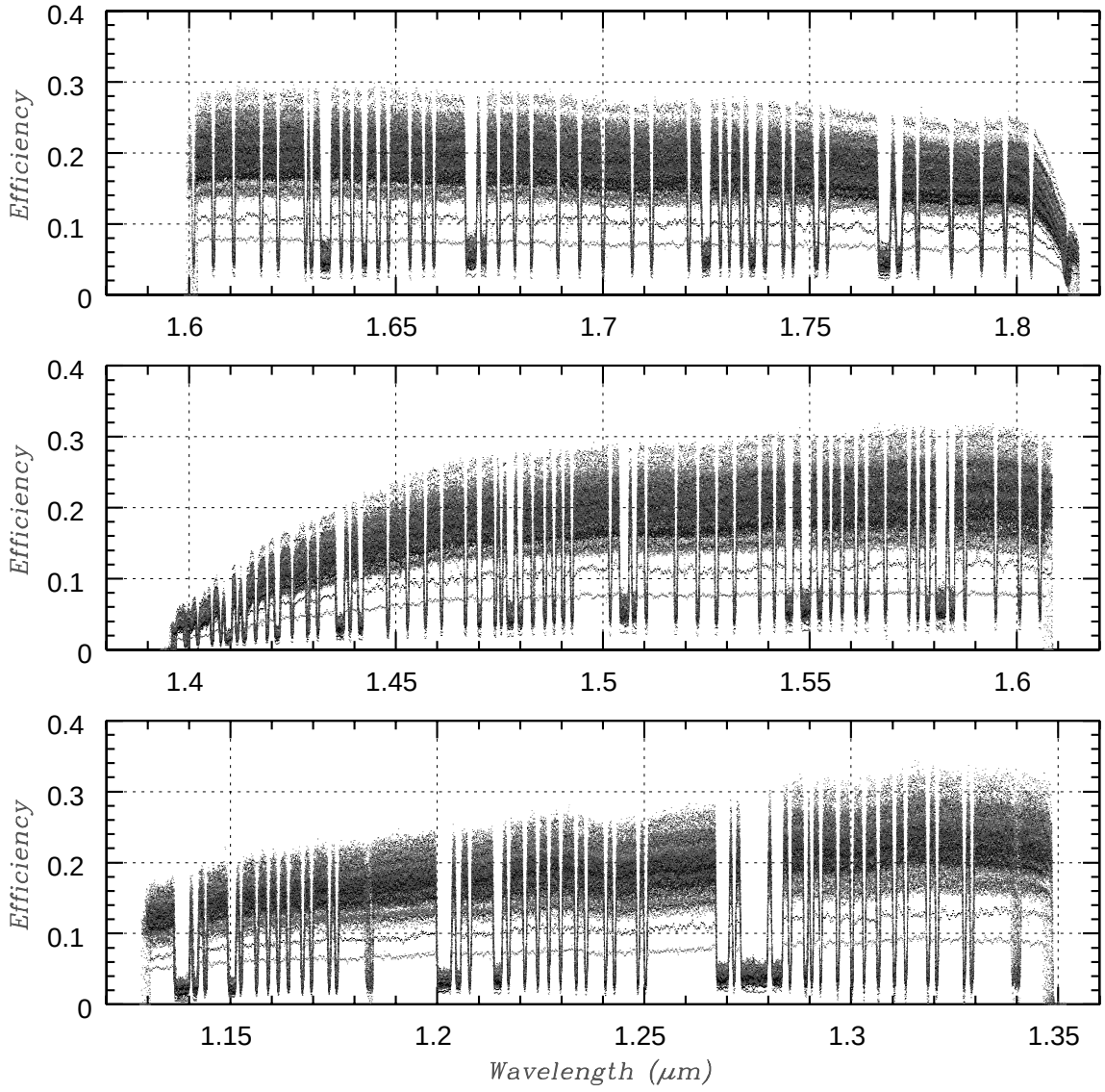

Figure 5. Absolute efficiencies of the system from the prime focus corrector to the detector in the J-long (bottom), H-short (middle), and H-long (top) wavelength range. The quantum efficiency of the detector is included.

Here, we assume the maximum throughput of the refractive optical elements (including two fibers) is 0.96, reflectivity of the mirrors is 0.98, and the filter throughput, efficiency of the reflective grating, and the detector quantum efficiency are 0.9 each. The conversion factor of the detector readout electronics of IRS1 replaced recently is 2.1 electrons/ADU, which was measured using a temporal light source in the refrigerator. Although this value is estimated by a little bit rough measurement, the detected photon counts by IRS1 and IRS2 in this efficiency test are almost the same value (the difference is less than 5%), indicating that there are no serious problem on the efficiency of each spectrograph. The gradual absorption feature from 1.5μm to 1.4μm is due to the attenuation of the fiber (9dB/km or 88%/60m) and possible slight water condensation on the optical surface in the spectrograph. Further investigations are required to make all the contributions to this absorption clear.

The distributions of the relative efficiency of the fibers in each wavelength range is represented as three

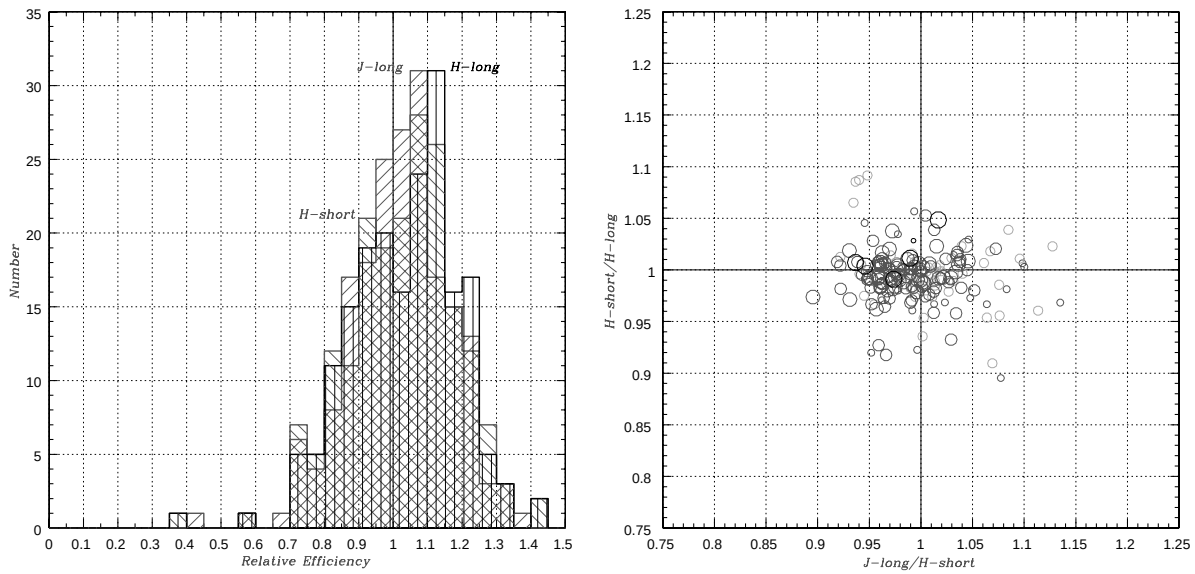

Figure 6. Distribution histograms of the relative efficiencies (left). The distributions in the J-long (1.13∼1.35μm), H-short (1.4∼1.6μm), and H-long (1.6∼1.8μm) are overplotted in the same diagram. The efficiencies are normalized by the averaged value in each band. Ratio of the relative efficiencies among two bands (right). The size of the symbol represents the relative efficiencies, larger symbols denote higher efficiencies.

histograms in Fig. 6. In this distribution, the effect of the ununiformity of the detector quantum efficiency has been removed by the thermal flat image taken under the ambient temperature condition. There are no wavelength dependencies in the distribution, the mode value (~ 1.1) is 10% higher than the average and 80% of the maximum efficiency (~ 1.4). There are two fibers having very low throughputs, which can also be identified in the Fig. 4. The uniformity of the wavelength dependency of the relative throughput is shown in the right panel of Fig. 6. Although there is a marginal tendency that the lower throughput fibers have relatively higher throughput in the J-long band, the global characteristics seems almost the same with 10% scattering.

After the check of the total system efficiency, the engineering observation was carried out. As explained in section 2, we adjusted the position of the corrector lenses to the optical axis of the telescope, before we determined the positions of the rotator axis and the distortion center (i.e. the optical axis of the telescope). The typical FWHM of the point source under the usual seeing condition is $0\farcs8$ arcsec in the optical wavelength of 0.7μm. The aberration coefficient estimated from the Shack-Hartmann image indicates that the spherical and the coma aberration is small enough, while the astigmatism component contributes to the image size of $\sim 0\farcs4$ even at the center of the field. As a result of these measurement, we conclude that the corrector lens system has no serious problems except for the astigmatism component probably caused by the unoptimized parameter of the primary mirror control matrix. The position difference between the rotator axis and the distortion center is $\sim$ 4.3mm, which causes $0\farcs25$ shift at the outer edge region of f.o.v. for 13° rotation of the instrument rotator. Consequently, we have to readjust ("tweak") a part of the outer fibers between long exposures. No tilt of the focal plane was detected in this measurement.

Next, an open cluster was observed to test the auto-guide using the guide fiber bundles as well as to check the position accuracy of the science fibers. Fig. 7 shows the image of the guide fiber bundles aiming 9 guide stars. The position error of the telescope is calculated by the weighted average of the position offsets of these stars. Auto-guiding using a star in Fig. 7 was succeeded.

Fig. 8 are the first light images obtained by IRS1 in the J-long and the H-short bands. In these images, there are many strong airglow lines because the airglow mask has not been aligned yet. Although we tried to check the image size of the point sources on the science fibers by giving small offsets to the field, we could only

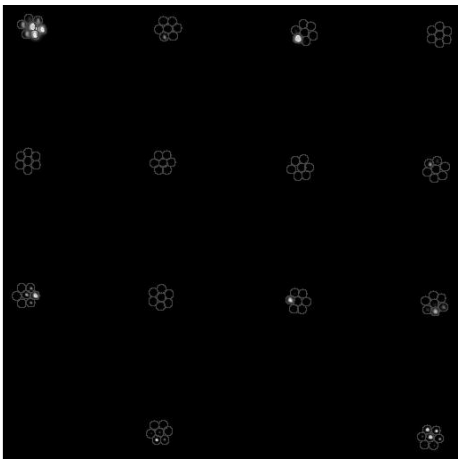

Figure 7. The image of the fiber bundles for auto-guiding of the telescope. All the guide stars will be captured at the center of each bundle, when all the parameters in the Echidna control software are fixed.

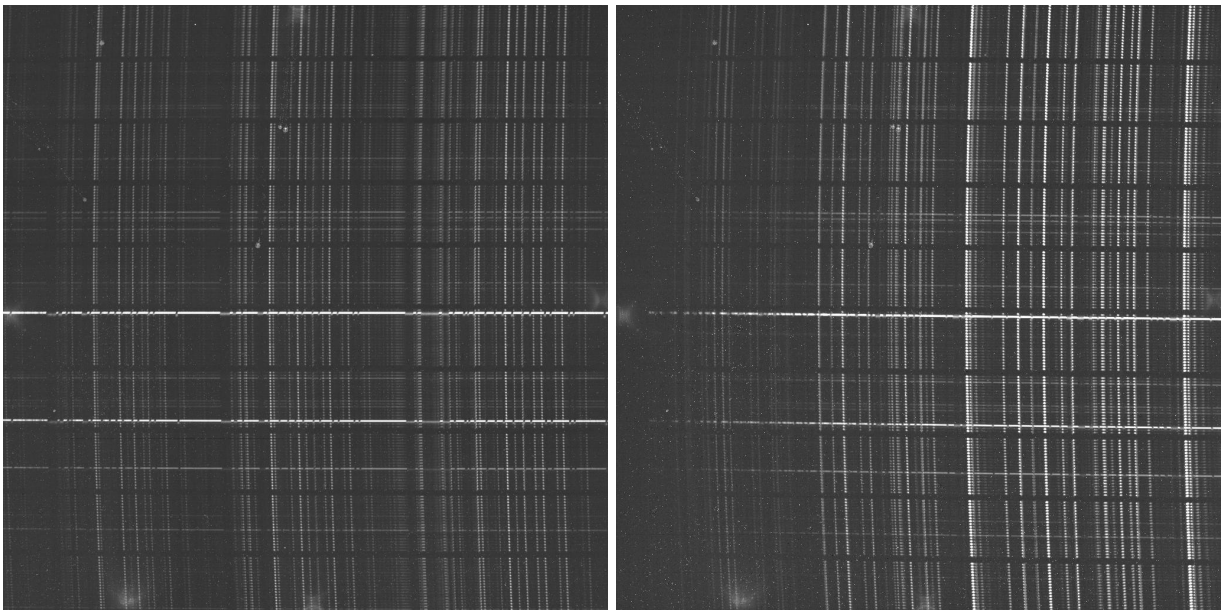

Figure 8. The spectra of stars with the airglow emission lines in the J-long (left) and the H-short (right) bands. The airglow mask has not been aligned yet.

confirm the image size may be almost the same as the fiber diameter, owing to unstable telescope response. The precise measurement will be done in the next engineering observation.

4. DISCUSSION

Three engineering observation runs of FMOS have already been finished. While the test process was not always carried out smoothly, almost all the results are acceptable without any serious problems. Followings are the summary of the troubles discovered in the past engineering runs and the expected solution.

1. The origin of the absorption feature between 1.4 and 1.5μm has not been resolved completely. We need to monitor the amount of this absorption feature to determine whether the major origin is slight water condensation on the optical surface in the spectrograph or not.

2. The astigmatism component of $\sim 0''.4$ will be reduced after the mirror analysis of the telescope in detail.

3. The position difference between the rotator axis and the distortion center cannot be fixed, because these positions are based on the structure of the telescope itself. We operate the Echidna to compensate the position shift by tweaking the fibers in the outer field between long exposures.

4. When all the guide stars will be captured at the center of each bundle after the completion of the Echidna parameter setting, we can give the small offset to the telescope by adding the offset value to the error amount detected by the guide bundle images. The accurate focus position and the image size will be investigated using the fiber auto-guide with a small internal offset.

5. We have to adjust the optical components as well as the control parameters of two spectrographs. The current work on these spectrographs is mainly in the J-long or H-short bands, while there are still many work in the other observation mode of the spectrographs.

The engineering runs are scheduled in June, August, and October in this year, and will be completed in the early 2009.

REFERENCES

[1] Maihara, T., Ohta, K., Tamura, N., Ohtani, H., Akiyama, M., Noumaru, J., Kaifu, N., Karoji, H., Iye, M., Dalton, G. B., Parry, I. R., Robertson, D. J., Sharples, R. M., Ren, D., Allington-Smith, J. R., Taylor, K., and Gillingham, P. R., "Fiber multi-object spectrograph (fmos) for the subaru telescope," in [*Optical and IR Telescope Instrumentation and Detectors*], Iye, M. and Moorwood, A. F., eds., *Proc. SPIE* **4008**, 1111–1118 (2000).

[2] Kimura, M., Maihara, T., Ohta, K., Iwamuro, F., Eto, S., Lino, M., Mochida, D., Shima, T., Karoji, H., Noumaru, J., Akiyama, M., Brzeski, J., Gillingham, P. R., Moore, A. M., Smith, G., Dalton, G. B., Tosh, I. A., Murray, G. J., Robertson, D. J., and Tamura, N., "Fibre-multi-object spectrograph (fmos) for subaru telescope," in [*Instrument Design and Performance for Optical/Infrared Ground-based Telescopes*], Iye, M. and Moorwood, A. F., eds., *Proc. SPIE* **4841**, 974–984 (2003).

[3] Eto, S., Maihara, T., Ohta, K., Iwamuro, F., Kimura, M., Mochida, D., Wada, S., Imai, S., Narita, Y., Nakajima, Y., Karoji, H., Noumaru, J., Akiyama, M., Gillingham, P., Smedley, S., and Tamura, N., "The fiber multi-object spectrograph (fmos) for the subaru telescope iii," in [*Ground-based Instrumentation for Astronomy*], Moorwood, A. F. and Iye, M., eds., *Proc. SPIE* **5492**, 1314–1318 (2004).

[4] Kimura, M., Maihara, T., Iwamuro, F., Eto, S., Akiyama, M., Ohta, K., Sakai, M., Tamura, N., and Mochida, D., "Fmos: The fiber multi-object spectrograph v results of early pir engineering run," in [*Ground-based and Airborne Instrumentation for Astronomy*], McLean, I. S. and Iye, M., eds., *Proc. SPIE* **6269**, 132–137 (2006).

[5] Gillingham, P. R., Miziarski, S., Akiyama, M., and Klocke, V., "Echidna: a multifiber positioner for the subaru prime focus," in [*Optical and IR Telescope Instrumentation and Detectors*], Iye, M. and Moorwood, A. F., eds., *Proc. SPIE* **4008**, 1395–1403 (2000).

[6] Moore, A. M., Gillingham, P. R., Griesbach, J. S., and Akiyama, M., "Spine development for the echidna fiber positioner," in [*Instrument Design and Performance for Optical/Infrared Ground-based Telescopes*], Iye, M. and Moorwood, A. F., eds., *Proc. SPIE* **4841**, 1429–1439 (2003).

[7] Gillingham, P., Correll, D., Dawson, J., Moore, A. M., Muller, R., Smedley, S., and Smith, G. A., "Echidna: the engineering challenges," in [*Ground-based Instrumentation for Astronomy*], Moorwood, A. F. and Iye, M., eds., *Proc. SPIE* **5492**, 1228–1242 (2004).

[8] Gillingham, P. R., Moore, A. M., Akiyama, M., Brzeski, J., Correll, D., Dawson, J., Farrell, T. J., Frost, G., Griesbach, J. S., Haynes, R., Jones, D., Miziarski, S., Muller, R., Smedley, S., Smith, G., Waller, L. G., Noakes, K., and Arridge, C., "The fiber multi-object spectrograph (fmos) project: the anglo-australian observatory role," in [*Instrument Design and Performance for Optical/Infrared Ground-based Telescopes*], Iye, M. and Moorwood, A. F., eds., *Proc. SPIE* **4841**, 985–996 (2003).

[9] Murray, G. J., Dodsworth, G. N., Content, R., Tamura, N., Robertson, D. J., Gedge, D., and Brooks, B., "An ultraprecision fiber connector for fmos," in [*Ground-based Instrumentation for Astronomy*], Moorwood, A. F. and Iye, M., eds., *Proc. SPIE* **5492**, 1383–1394 (2004).

[10] Iwamuro, F., Maihara, T., Ohta, K., Eto, S., Sakai, M., Akiyama, M., Kimura, M., Tamura, N., Noumaru, J., Karoji, H., Dolton, G. B., Lewis, I. J., Tosh, I. A. J., Murray, G. J., Dipper, N. A., Robertoson, D. J., Gillingham, P. R., Smedley, S., Smith, G. A., and Frost, G., "Fmos - the fiber multiple-object spectrograph iv: current status of ohs-based spectrograph," in [*Ground-based and Airborne Instrumentation for Astronomy*], McLean, I. S. and Iye, M., eds., *Proc. SPIE* **6269**, 43–50 (2006).

[11] Lewis, I. J., Dalton, G. B., Holmes, A. R., Brooks, B., Band, C., Tosh, I. A., Woodhouse, G. F., Cavan, N., Murray, G. J., Robertson, D. J., Dipper, N. A., and Luke, P., "Developments on the uk fmos project for the subaru telescope," in [*Instrument Design and Performance for Optical/Infrared Ground-based Telescopes*], Iye, M. and Moorwood, A. F., eds., *Proc. SPIE* **4841**, 1108–1114 (2003).

[12] Tosh, I. A., Woodhouse, G. F., Froud, T., Dowell, A., Patel, M., Wallner, M., Lewis, I. J., Dalton, G. B., Holmes, A., Brooks, B., Band, C., Bonfield, D. G., Murray, G. J., Robertson, D. J., and Dipper, N. A., "The current status of the uk-fmos spectrograph," in [*Ground-based Instrumentation for Astronomy*], Moorwood, A. F. and Iye, M., eds., *Proc. SPIE* **5492**, 1362–1370 (2004).

[13] Dalton, G. B., Lewis, I. J., Bonfield, D. G., Holmes, A. R., Brooks, C. B., Lee, H., Tosh, I. A. J., Froud, T. R., Patel, M., Dipper, N. A., and Blackburn, C., "The uk fmos spectrograph," in [*Ground-based and Airborne Instrumentation for Astronomy*], McLean, I. S. and Iye, M., eds., *Proc. SPIE* **6269**, 136–145 (2006).